HONGFEN ZHANG
XIANGFENG SHI
ERXIN GAO
SHAOFEI ZHAO
and
RUIHONG ZHANG

Study on the pore structure evolution and fractal feature in the process of spontaneous combusiton of coal

This paper studies the variation of pore structure of coal and the fractal law of pores in two-dimensional and three-dimensional space in coal spontaneous combustion using scanning electron microscope and mercury injection experiment. The pore structure of coal changes slowly during 30ºC-200ºC and there is a great change during 200ºC-300ºC. The most probable pore size is about 5nm during 30ºC-200ºC and micropore and transitional pore are dominating. The most probable pore size reaches 310nm at 300ºC and macropores and mesopores are dominating during 200ºC-300ºC. During coal spontaneous combustion, the total pore volume and porosity rise gradually, the specific surface area of pores first rises and then goes down, the permeability goes down first then rises sharply and then goes down, the diameter of the pore with fractal feature gradually goes up and the fractal feature is more and more obvious. Both in two-dimensional and three-dimensional spaces, the fractal dimension of the pore enlarges gradually, indicating that the surface of the coal is becoming more and more coarse and the pore structure is gradually uniform, and the growth rate of fine pore is faster than that of macro pore.

Keywords: *Coal spontaneous combustion, pore structure, SEM, mercury injection, fractal dimension.*

1. Introduction

Coal is a typical non-uniform porous medium, and its pore structure determines the adsorptivity and fluidity of gas in coal [1-7], which has a crucial influence on its spontaneous combustion characteristics [8]. A large number of studies show that the pore distribution of porous media satisfies self-similarity and conforms to the fractal law [9-11]. In recent years, scholars have conducted researches on the pore structure and fractal feature of coal using various experimental methods such as synchrotron radiation small-angle X-ray scattering (SAXS) [12], broad ion beam-scanning electron microscope imaging (BIB-SEM) [13], CT [14], small-angle rays and canning electron microscope combining [15]. However, current study does not involve the change of coal sample temperature, and there are few studies on the pore structure change and fractal characteristics of coal during its spontaneous combustion. Wang Yi et al. studied the evolution characteristics of pore structure in the process of spontaneous combustion of coal seam [16-17]. However, the research was aimed at the temperature range of 300ºC-600ºC, and the conclusion drawn is not appropriate for coal spontaneous combustion. In order to obtain the change rule of pore structure in coal spontaneous combustion process, the author used SEM and mercury injection experiment to measure the pore structure of coal sample at different temperatures in the spontaneous combustion of the coal. Through scanning the shape of the surface grain of the coal sample using scanning electron microscope and analyzing the topological structure of the pore using the mercury injection experiment, this paper gradually reveals the law and change of coal pore structure during coal spontaneous combustion, which provides basic data for promoting the secure and efficient mining of coal and preventing coal spontaneous combustion accidents.

Messrs. Hongfen Zhang, Xiangfeng Shi, Shaofei Zhao and Ruihong Zhang, Architectural Engineering College, North China Institute of Science and Technology, Langfang 065 201 and Erxin Gao, School of Mechanics and Civil Engineering, China University of Mining and Technology (Beijing), Beijing 100 083, China. E-mail: zhfkd@sina.com

2. Determination of SEM image and fractal dimension in the coal spontaneous combustion process

2.1 Sample preparation

The experimental coal sample is collected from the soft coal No.2 coal seam of Zaoquan coal mine. No.2 coal seam is a type-II spontaneous combustion coal seam. The experimental results of coal sample industrial analysis and elemental analysis are shown in Table 1. In the experiment, the coal sample was first broken into lumps with the particle size smaller than 25mm and the lumps were divided into three groups. Each group of coal samples was put into the muffle furnace in a proper order. The final temperature was set as

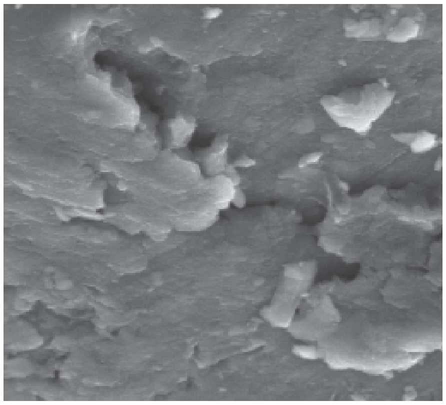

Fig.1 SEM image of coal sample at the temperature of 100^{o}C

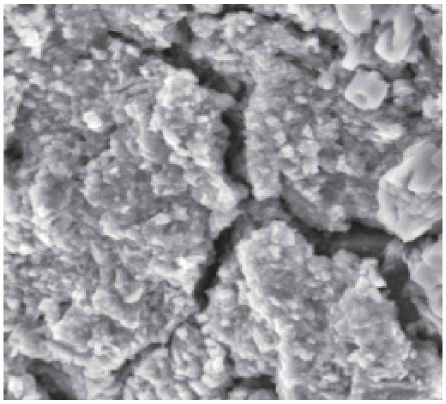

Fig.2 SEM image of coal sample at the temperature of 200^{o}C

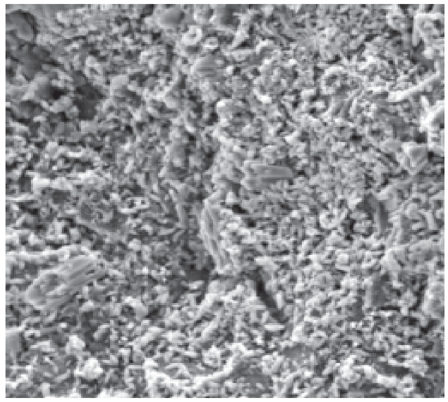

Fig.3 SEM image of coal sample at the temperature of 300^{o}C

TABLE 1: INDUSTRIAL ANALYSIS AND ELEMENTAL ANALYSIS DATA OF EXPERIMENTAL COAL SAMPLES

V_{ad} /%	A_{ad} /%	C_{ad} /%	St_{ad} /%	H_{ad} /%	O_{ad} /%
22.98	18.9	67.13	0.47	3.62	7.70

100^{o}C, 200^{o}C and 300^{o}C respectively. The samples were heated up to the final temperature and after two hours, they were taken out and cooled down to the room temperature. Many tiny fragments were clamped down from the edge of the coal sample. The flakelets with relatively flat natural cross sections were selected as the observation samples. The surface adhesive materials were blown away by a suction bulb. Then, the coal sample was coated with Gatan682-type ion etching thin-film deposition equipment for standby application.

2.2 DETERMINATION OF SEM IMAGE AND FRACTAL DIMENSION

In this experiment, the microstructure of the coal sample surface was observed by the MERLIN compact ultrahigh resolution field-emission scanning electron microscope from the Center of Scanning Electron Microscopy of Tsinghua University.

The coal samples at different temperature were observed by the scanning electron microscopy. When the magnification is 10,000, the surface of the coal sample is as shown in Figs.1, 2 and 3. There is obvious difference in the surface morphology of the coal sample at different temperatures. With the rise of the temperature, the number of pore fissures grew sharply and the surface of the coal sample became rough gradually.

Figs.1, 2 and 3 show that the surface of the coal sample is porous, uneven and disorganized, which is hard to be described using traditional Euclid theory. A large number of studies both at home and abroad show that coal is a kind of fractal particle, which can be quantitively portrayed by fractal dimension. More than a dozen of different dimensions, such as Hausdorff dimension, topological dimension, information dimension, self-similarity dimension, and correlation dimension have been developed so far since the fractal theory was established by Mandelbrot in the 1970s[18]. Based on the SEM imaging, this paper carries out a quantitative analysis of the pore distribution characteristics on the coal surface using Hausdorff dimension, i.e. Box-counting dimension.

The definition of fractal box-counting dimension is as follows: Assume that A is an arbitrary non-null bounded subset in the space of R^n. When r is larger than 0, a minimum of $N_r(A)$ n-dimension cubes with the side length r are required to cover A. If there is d, when r approaches to 0, we have:

$$N_r(A) \propto 1/r^d \quad \text{... (1)}$$

Then, d is called the box-counting dimension of A. At this time, there is only one positive number k, which makes

$$\lim_{r\to 0} \frac{N_r(A)}{1/r^d} = k \quad \text{... (2)}$$

Take the logarithm to both side of equation (2), and we have:

$$d = \lim_{r\to 0} \frac{\lg k - \lg N_r(A)}{\lg r} = -\lim_{r\to 0} \frac{\lg N_r(A)}{\lg r} \quad \text{... (3)}$$

In the calculation process, the number $N_r(A)$ of boxes required to cover A at different r values were figured out. The points were converged in the semi-logarithmic coordinate system with lgr as the x-coordinate and $lgN_r(A)$ as the y-coordinate. Finally, the absolute value of the gradient of the fit lines through these points were figured out, which is the box-counting dimension of the set A.

Take the SEM image (Fig.2) at 200^{o}C as an example. Fig.2 was transformed to a black-and-white binary image (Fig.4) after a proper threshold value was selected. Boxes with the side length of r was selected to cover the image area, as shown in Fig.5. The box-counting dimension can be figured out using formula (3) after the quantity of boxes containing pores was figured out.

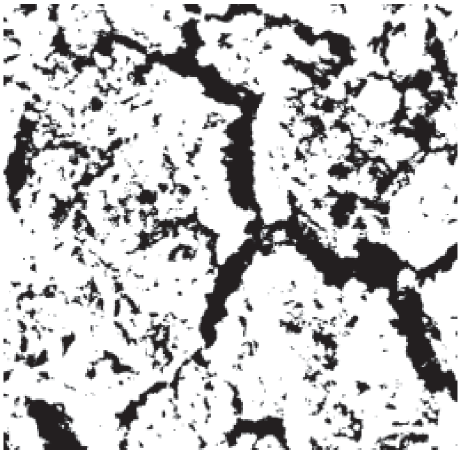

Fig.4 Binary image corresponding to Fig.2

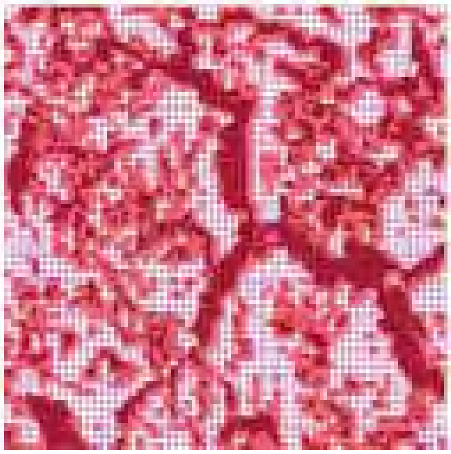

Fig.5 Diagram of coverage of pores and fissures by the gridding with certain side length

The calculation results of pore distribution box-counting dimension of the coal sample at different temperatures are shown in Figs.6, 7 and 8. It can be seen that the degree of fitting of the coal samples at different temperatures is fairly high (R^2>0. 99), suggesting that the coal samples have obvious fractal features. The box-counting dimension of the coal sample is 1.512, 1.783 and 1.916 at the temperature of 100°C, 200°C and 300°C respectively. As the temperature rose, the box-counting dimension became larger, suggesting that the surface of the coal sample is getting rougher and rougher, the specific surface area is becoming bigger and bigger and the adsorption capacity is stronger and stronger[19].

3. Changes of coal pore structure and coal fractal characteristics in the spontaneous combustion

3.1 Mercury injection experiment

The experimental coal sample is the soft coal collected from Zaoquan coal mine No. 2 coal seam. The lump coal was firstly smashed to the coal grains with a diameter of 2cm. Then the coal sample was put into an oxidation tank with constant temperature. The temperature of the oxidation tank was set as 30°C, 100°C, 200°C and 300°C successively. The sample was kept for 12 hours at each temperature, and then was taken out and put into a dry glass bottle to be sealed. About 2g coal sample at each temperature was taken out in sequence for the mercury injection experiment.

The experiment equipment is AutoPore IV series mercury injection apparatus, with the aperture measurement range of 0.003-1100μm. The peak pressure is 60,000 *psia*. The mercury injection and withdrawal volume is precise, which is superior to 0.1μL.

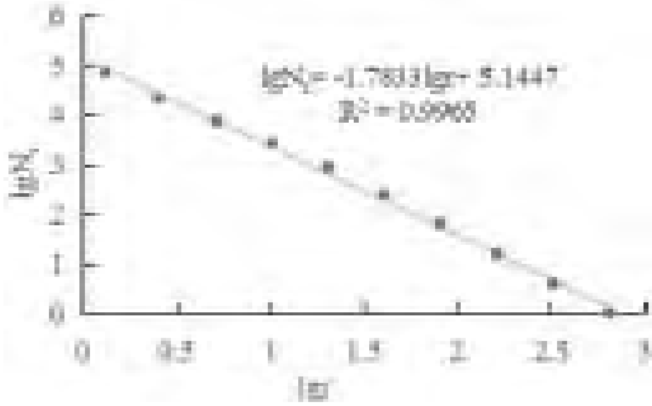

Fig.7 $lgN_r(A)$-lgr fitting straight-line of the pores and fissures of coal sample at 200°C

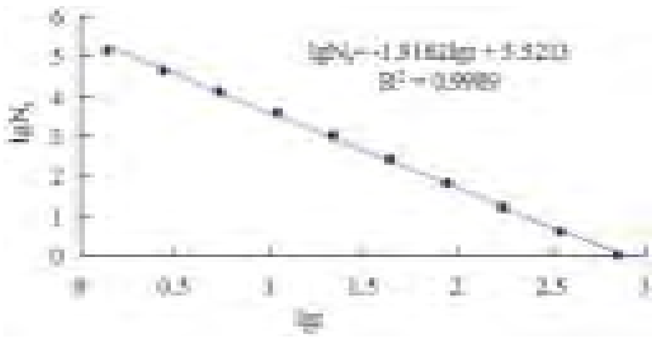

Fig.8 $lgN_r(A)$-lgr fitting straight-line of the pores and fissures of coal sample at 300°C

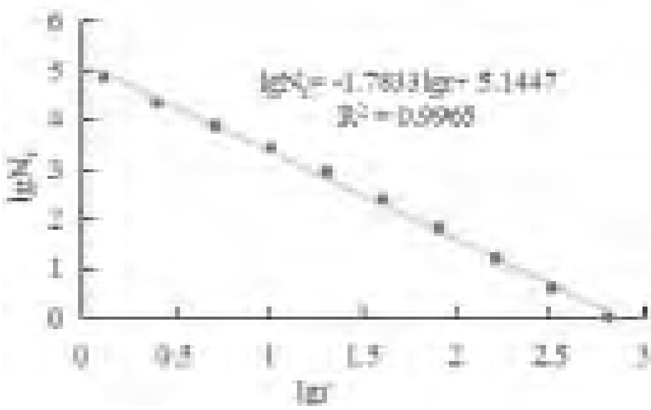

Fig.6. $lgN_r(A)$-lgr fitting straight-line of the pores and fissures of coal sample at 100°C

3.2 Change rule of the pore structure of the coal sample in its spontaneous combustion

The distribution of the pore diameters of the coal sample in its spontaneous combustion is shown as follows. This distribution is obtained from the mercury injection experiment. In the figure, *D* refers to the pore diameter and *Dv* means the pore volume increment.

It can be seen from the above figure that, the distribution range of the pore diameters of the experimental coal samples is very large. The minimum pore diameter is just several nms, while the maximum pore diameter is approaching 350,000nm. The pore structure is rather complicated, including micropores, transitional pores, mesopores, and macropores. As a whole, as the temperature rose, the pore structure of the coal was changing constantly. There were slow changes in the pore structure before 200°C, but it changed sharply between 200°C and 300°C. The distribution diagrams at 30°C, 100°C and 200°C are similar, each having two obvious peaks. And each peak is corresponding to the pore diameters of 4nm and 100nm. What is different is that the most probable pore size of the coal sample at 30°C, 100°C and 200°C declined somewhat with the rise of temperature and that the number of the most probable pore was obviously increasing.The distribution diagram of the pore diameter of the coal sample at 300°C is obviously different from those of the coal sample at 30°C, 100°C and 200°C. The most probable pore size is 310nm. The number of micro holes and transition holes reduced significantly, while the number of macropores and mesopores increased greatly. The pore structure parameters at different temperature in the process of coal spontaneous combustion obtained by the mercury experiment are as shown in Table 2. Xonot defined pore size classification method is adopted here. D refers to the pore diameter (for large pore, the diameter is larger than 1,000nm; for mesopore, the diameter is larger than 100nm and smaller than 1,000nm; for transitional pore, the diameter is larger than 10nm and smaller than 100nm; for micropore, the diameter is smaller than 10nm.)

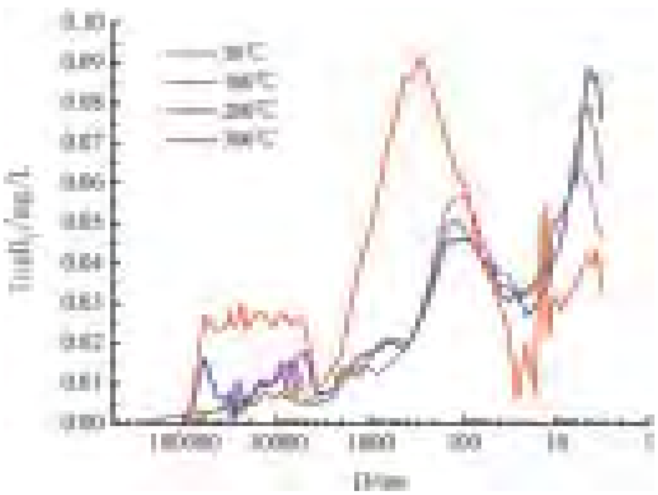

Fig.9 The distribution diagram of pore diameters of the coal sample at 30°C, 100°C, 200°C and 300°C

It can be seen from Table 2 that the transitional pore takes up the largest proportion in the coal sample at 30°C, which is followed by the micropore. The two kinds of pores account for 62% of the pore volume. When the temperature rises to 300°C, the percentage of macropore and mesopore dominates the advantage, which remains at 74%. During this period of time, the pore structure is changing constantly.

TABLE 2: MERCURY JNJECTION EXPERIMENTAL DATA OF THE COAL SAMPLE AT DIFFERENT TEMPERATURE IN THE COAL SPONTANEOUS COMBUSTION PROCESS

Parameter	30°C	100°C	200°C	300°C
V_1/V_Z/%	25	30	30	10
V_2/V_Z/%	36	32	27	16
V_3/V_Z/%	24	25	21	38
V_4/V_Z/%	15	13	22	36
V_Z/mL/g	0.118	0.124	0.137	0.188
Porosity/%	14.708	15.324	16.041	22.001
Average pore diameter/nm	17.7	14.6	15.2	41.0
Total pore area/m^2/g	26.702	34.182	36.210	18.350
Permeability /mdarcy	11.165	4.127	80.485	76.575
Tortuosity	10.138	16.274	8.054	10.958

Note: V_z is the total pore volume; V_1 is the micro pore volume; V_2 is the transitional pore volume, V_3 is the mesopore volume and V_4 is the macropore volume.

It is the phase of water evaporation and gas desorption between 30°C and 100°C. The evaporation of water and the desorption of gas are constantly speeding up the generation of small pores in the coal, making the proportion of the micropores increase. The proportion of transition pore is decreasing, while the proportion of mesopore and macropore is almost constant. Meanwhile, affected by the increase of the micropore, the specific surface area of the pore grew from 26.702 m^2/g to 34.182m^2/g and the average porous diameter decreased from 17.7nm to 14.6nm. During this period, the total pore volume increased from 0.118ml/g to 0.124ml/g. The tortuosity of the pore passage grew from 10.138 to 16.274. Affected by the increase of tortuosity and the Klinkenberg effect aroused by the slippage viscosity of gas, the permeability declined from 11.165 to 4.127. When the temperature is between 100°C and 200°C, the total pore volume, porosity, total pore surface area, and average porous diameter are all increasing. The permeability underwent the most obvious change. Affected by the decline of the tortuosity of the pore passage and the disappear of the Klinkenberg effect, the permeability increased sharply from 4.127 to 80.485.

From 200°C to 300°C, the change of the pore structure is the most obvious. The proportion of mesopores and macropores rose sharply, while the proportion of micropore and transitional pore declined dramatically, which changed the previous pattern dominated by micropore and transitional pore. Within this temperature range, the total pore size volume increased from 0.137ml/g to 0.188ml/g, the porosity grew from 16.041% to 22.001%, the average porous diameter rose from 15.2nm to 41.0nm and the tortuosity of the pore passage went up from 8.054 to 10.958, while the penetration rate decreased from 80.485 to 76.575. The reason behind these changes is that with the rise of the temperature, the coal oxygen composite reaction became stronger and stronger. Methane, carbon monoxide, carbon dioxide and other gases were releasing at a quicker speed, generating new pore fissures. The anisotropy in the expansion of new and old pore fissures can produce stress concentration locally. When the stress is higher than the intensity of coal sample, various fractures will come into being. The fractures made the pore volume expand obviously. The pore structure is getting more and more complicated and the seepage channels became more and more twisty.

In a word, in the process of coal spontaneous combustion, the micropores and transition pores are dominant at low temperature, and the pore structure with mesopores and macropores gradually developed with the increase of temperature. The total pore volume and porosity increased with the rise of temperature, and the specific surface area of the pore rose first and then declined in the spontaneous combustion of the coal under the control of micropore volume percentage value. Affected by the Klinkenberg effect and the tortuosity of the pore passage, the penetration rate decreased with the increase of the temperature, then rose sharply and then decreased.

3.3 Change rule of coal pore fractal characteristics during spontaneous combustion

The following relational expression can be obtained based on the basic definition of fractal theory [20]:

$$n(r) = n_0 (r/r_0)^{-D} \quad \text{...} \quad (4)$$

where:

r - pore radius;

r_0 - maximum pore radius;

n_0 - the quantity of pore with the maximum pore radius r_0;

D - fractal dimension;

$n(r)$ - number of pores whose diameter is not smaller than r.

Perform differential calculation on r at each side of formula (4) and the following equation is obtained:

$$dn = -n_0 r_o^D D r^{-(D+1)} dr \quad \text{...} \quad (5)$$

The total volumed $V(r)$ of the pore with a radius of r-$r+dr$ can be expressed as follows:

$$dV(r) = \frac{3}{4}\pi r^3 dn(r) \quad \text{...} \quad (6)$$

where, $V(r)$ - the total volume of pore with the radius not smaller than r.

Substitute (5) into formula (6) and the following equation is obtained:

$$dV(r) = -\frac{3}{4}\pi n_0 r_0^D D r^{2-D} dr \quad \text{...} \quad (7)$$

Perform differential calculation on r at each side of formula (7) and the following equation is obtained:

$$V_0 - V(r) = \frac{\frac{3}{4}\pi n_0 r_o^D D}{3-D} r^{3-D} \quad \text{...} \quad (8)$$

where, V_0 is the total volume of the coal pore. Let $V_0 = V(0)$.

In the mercury penetration experiment, in order to overcome the internal surface tension between mercury and solid, the mercury injection pressure $P(r)$ and the pore radius r must satisfy certain relationship. Based on the Washburn equation, we have:

$$P(r) = \frac{2\sigma \cos\theta}{r} \quad \text{...} \quad (9)$$

where, σ - surface tension of the mercury; let σ = 0.48N/m; θ - the wetting angle between mercury and coal body; let θ =140^o

Substitute formula (9) into (8) and we have:

$$V_0 - V(r) = \frac{\frac{3}{4}\pi D(2\sigma\cos\theta)^{3-D} n_o r_o^D}{3-D} P^{D-3}(r) = KP^{D-3}(r) \text{...} \quad (10)$$

For the given coal sample, K is a constant.

Take the logarithm at each side of formula (10), and we have:

$$\lg[V_0 - V(r)] = (D-3)\lg P(r) + \lg K \quad \text{...} \quad (11)$$

It is possible to find out whether the pore structure of coal has fractal features after confirming if there is a linear relation between lg[V_0-$V(r)$] and lg$P(r)$ in the dual-logarithm coordinates system. If there is a linear relationship between the two, based on the value k of the slope, the fractal dimension can be figured out, which is D = 3+k. However, the fractal in the nature is mostly not complete fractal, but the fractal within certain range. Based on the mercury injection experiment data, the fitting result of the pore fractional dimension within the pore-size range are figured out and are shown as follows (Figs.10-13):

It is learned from Figs.10, 11, 12 and 13 that the slope of the fitting straight line at 30^{o}C, 100^{o}C, 200^{o}C and 300^{o}C is -0.169, -0.129, -0.068 and -0.067 respectively. The fractal dimension of the coal sample at different temperature was figured out according to formula (11) and the results are shown in Table 3.

It can be seen from Table 3 that in the coal spontaneous combustion, the radius range of pores with fractal features is

Table 3: Pore fractal dimension table of coal sample at different temperatures

Temperature /^{o}C	Aperture range /nm	Fractal dimension
30	14-8051	2.831
100	17-15436	2.871
200	120-31056	2.932
300	1314-34169	2.933

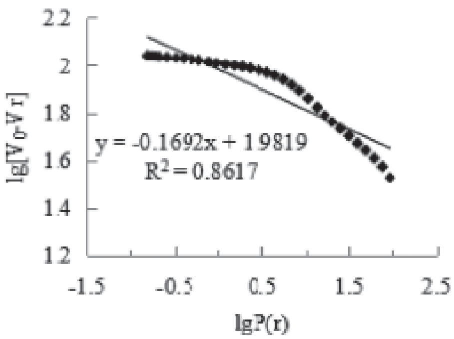

Fig.10 Fitting straight line of the fractal dimension of coal pores at 30°C

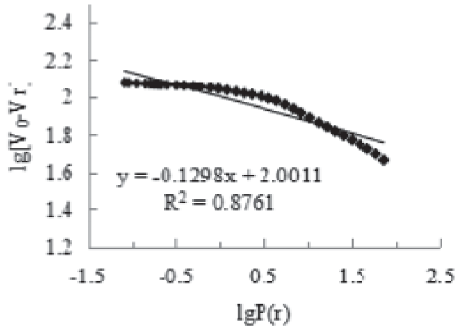

Fig.11 Fitting straight line of the fractal dimension of coal pores at 100°C

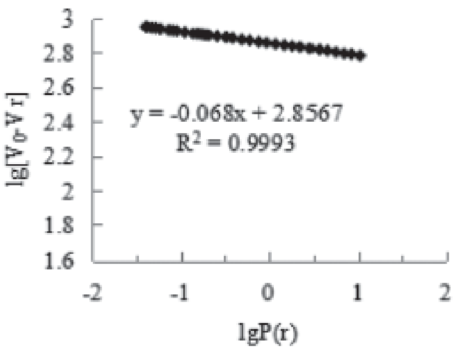

Fig.12 Fitting straight line of the fractal dimension of coal pores at 200°C

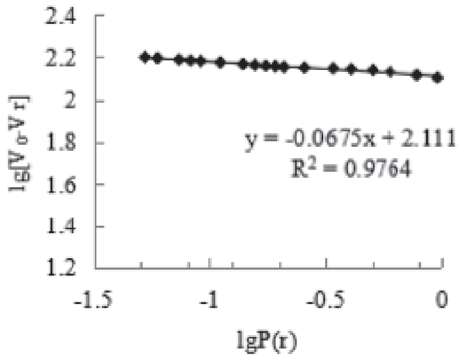

Fig.13 Fitting straight line of the fractal dimension of coal pores at 300°C

getting larger and larger and the pore fractal dimension of the coal is becoming larger and larger, suggesting that the pore fractal feature becomes more and more obvious with the rise of temperature and that the pore structure is becoming more and more balanced. In addition, it also indicates that the expansion of small pores is faster than that of large pores.

4. Conclusions

(1) It is learned from the SEM experimental study that there is obvious fractal feature on the surface of the coal sample in its spontaneous combustion. With the rise of temperature, the fractal dimension on the surface of coal sample becomes larger gradually.

(2) The mercury injection experiment shows that the distribution range of the pore diameters of the coal sample during its spontaneous combustion is very large. The pore structure is rather complicated, including micropores, transitional pores, mesopores, and macropores. As a whole, as the temperature rose, the pore structure of the coal was changing constantly. There were slow changes in the pore structure before 200°C, but it changed sharply between 200°C and 300°C. The most probable pore size of coal is about 5nm when the temperature is lower than 200°C and micropore and transitional pore are dominating. The most probable pore size of coal reaches 310nm at the temperature of 300°C and macropores and mesopores are dominating.

(3) The total pore volume and porosity increased with the rise of temperature, and the specific surface area of the pore rose first and then declined in the spontaneous combustion of the coal under the control of micropore volume percentage value. Affected by the Klinkenberg effect and the tortuosity of the pore passage, the penetration rate decreased with the increase of the temperature, then rose sharply and then decreased.

(4) In the coal spontaneous combustion, the radius range of pores with fractal features is getting larger and larger and the pore fractal dimension of the coal is becoming larger and larger, suggesting that the pore fractal feature becomes more and more obvious with the rise of temperature and that the pore structure is becoming more and more balanced. In addition, it also indicates that the expansion of small pores is faster than that of large pores.

Acknowledgment

This paper is one science and technology research project of institutions of higher education in Hebei province (project number:ZD2017314) and is a project supported by"the Fundamental Research Funds for the Central Universities" (project number: 3142017070).

References

1. Nie, B., Liu, X. and Yang, L. (2015): "Pore structure characterization of different rank coals using gas adsorption and scanningelectron microscopy," *Fuel*, Vol.158, pp.908-917, 2015.
2. An, F. H. and Cheng, Y. P. (2013): "The effect of small micropores on methane adsorption of coals from Northern China," *Adsorption-journal of the International Adsorption Society*, Vol. 19, No. 1, pp.83-90, 2013.
3. Osman, A. M. and Duwairi, H. M. (2015): "Forchheimer, non-Boussinseq natural convection in porous media filled enclosure," *International Journal of Heat and Technology*, vol.33, No. 4, pp.191-196, 2015.
4. Li, Q. Z., Lin, B. Q. and Wang, K. (2015): "Surface

properties of pulverized coal and its effects on coal mine methane adsorption behaviors under ambient conditions," *Powder Technology*, Vol. 270, pp. 278-286, 2015.

5. Nasser, L. and Duwairi, H. M. (2016): "Thermal dispersion effects on convection heat transfer in porous media with viscous dissipation," *International Journal of Heat and Technology*, Vol.34, No. 2, pp. 207-212, 2016.
6. Sun, W. J., Feng, Y. Y. and Jiang, C. F. (2015): "Fractal characterization and methane adsorption features of coal particles taken from shollow and deep coalmine layers," *Fuel*, Vol.155, pp.7-13, 2015.
7. Cai, Y., Liu, D. and Pan, Z. (2013): "Pore structure and its impact on CH4 adsorption capacity and flow capability of bituminous and subbituminous coals from Northeast China," *Fuel*, Vol. 103, pp.258-268, 2013.
8. Wang, H. Y., Cheng, Y. F. and Bo, Y. (2015): "Adsorption effect of overlying strata on carbon dioxide in coalfield fire area," *International Journal of Heat and Technology*, Vol. 33, No. 3, pp.11-18, 2015.
9. Xue, G. W., Liu, H. F. and Yao, H. F. 2011): "The types of tectonic coal and pore characters in Hancheng," *Journal of China Coal Society*, Vol.36, No. 11, pp.1845-1850, 2011.
10. Yao, Y., Liu, D. and Tang, D. (2008): "Fractal characterization of adsorption-pores of coals from North China:an investigation on CH adsorption capacity of coals," *International Journal of Coal Geology*, Vol.73, pp.27-42, 2008.
11. Li, X. J., Lin, B. Q. and Shi, T. H. (2013): "Experimental study on pore structuresof outburst coal andits adsorptionproperties at typical mining fields in Guizhou Province," *Journal of Mining & Safety Engineering*, Vol.30, No. 3, pp.415-420, 2013.
12. Zhao, Y. X., Liu, S. M. and Derek, E. (2014): "Pore structure characterization of coal by synchrotron small-angle xray scattering and transmission electron microscopy," *Energy & Fuels*, Vol. 28, No. 6, pp.3704-3711, 2014.
13. Giffin, S., Littke, R. and Klaver, J. (2013): "Application of BIB-SEM technology to characterize macropore morphology in coal," *International Journal of Coal Geology*, Vol. 114, No. 4, pp.85-95, 2013.
14. Peng, R. D., Yang, Y. C. and Ju, Y. (2011): "Computation of fractal dimension of rock pores based on gray CT images," *Chinese Science Bulletin*, Vol. 56, No. 31, pp.3346-3357, 2011.
15. Cai, Y. D., Liu, D. M. and Pan, Z. J. (2014): "Pore structure of selected chinese coals with heating and pressurization treatments," *Science China Earth Sciences*, Vol. 57, No. 7, pp.1567-1582, 2014.
16. Wang, Y., Zhao, Y. S. and Feng, Z. C. (2010): "Study of evolution characteristics of pore structure during flame coal pyrolysis," *Chinese Journal of Rock Mechanics and Engineering*, Vol. 29, No. 9, pp.1859-1866, 2010.
17. Wang, Y., Zhao, Y. S. and Feng, Z. C. (2010): "Evolution charactics of pore structure during lignite seam spontaneous combustion developing," *Journal of China Coal Society*, Vol. 35, No. 9, pp.1490-1495, 2010.
18. Peng, S. J., Xu, J. and Zhang, C. L. (2015): "Fractal characteristics of crack evolution in gas-bearing coal under shear loading," *Journal of China Coal Society*, Vol. 40, No. 4, pp.801-808, 2015.
19. Liu, A. H., Fu, X. H. and Liang, W. Q. (2013): "Pore distribution features of different rank coal and influences to coal bed methane development," *Coal Science and Technology*, Vol. 41, No. 4, pp.104-108, 2013.
20. Zhang, Y. T., Wang, D. M. and Zhong, X. X. (2007): "Features of fissure sharp in coal borehole and variation law with temperature," *Coal Science and Technology*, Vol. 35, No. 11, pp.73-76, 2007.